Autonomous Quadrotor Control: Virtual Application to the Surveillance of Endangered Animal Species

Journal:	*IET Control Theory & Applications*
Manuscript ID	CTA-2018-0102
Manuscript Type:	Regular Paper
Date Submitted by the Author:	26-Jan-2018
Complete List of Authors:	Kabir, Abdulmajeed; King Fahd University of Petroleum and Minerals, Systems Engineering Oyedeji, Mojeed; King Fahd University of Petroleum and Minerals, Systems Engineering Lasisi, Hammed; Osun State University, Electrical Engineering
Keyword:	Nonlinear Systems, System Modelling, System Simulation, Robotics

IET Research Journals

Submission Template for IET Research Journal Papers

IET Journals
The Institution of Engineering and Technology

Autonomous Quadrotor Control: Virtual Application to the Surveillance of Endangered Animal Species

ISSN 1751-8644
doi: 0000000000
www.ietdl.org

Abdulmajeed Muhammad Kabir[1*], *Mojeed Oyedeji*[1], *Lasisi Hammed*[2]

[1] *System Engineering Department, King Fahd University of Perturolem and Minerals, Dhahran, Saudi Arabia*
[2] *Osun State University, Osun State, Nigeria*
* *E-mail: kbmajeed1@gmail.com*

Abstract: In this work, we make use of the Backstepping and Proportional-Derivative (PD) methods for the control of a quadrotor unit and subsequently proposed for autonomous tracking of an endangered species; the 'Northern white rhino'. Extended Kalman Filter (EKF) estimation was applied for the localization of the rhino in a virtual wildlife reserve using a single collar sensor on the animal while a case of partial sensing was presented for energy saving considerations. The localization system sends the rhino's position trajectories to the quadrotor control system for tracking. This system has the potential to aid rangers, enhance surveillance, deter poachers and consequently help preserve endangered wildlife.

1 Introduction

Unmanned Aerial Vehicle (UAV) is a space-traversing vehicle that flies without a human pilot or crew and can be remotely controlled or can fly autonomously. There has been a sharp rise in the development, control and applications of quadrotors in recent years and the field of aerial robotics is fast-growing with engineers and hobbyists actively involved. A broad study on UAVs can be found in [1]. Quadrotors are small-sized, simple and highly maneuverable vehicles operating in three dimensional space, capable of translations and rotations resulting in six degrees of freedom. It is worthy of note that with four rotors as input actuators and six degrees of freedom, the quadrotor is an under-actuated system and as a result, there exists constraints in maneuvering. One main drawback in the use of quadrotors is power consumption. Hobbyist versions can remain airborne between ten and thirty minutes, however, there are new developments into powering these aircrafts with hybrid systems incorporating solar energy, combustion engines and the likes leading to airborne times of up to and more than one hour.

A serious problem in wildlife conservation exists in poaching, especially endangered species. The United Nations Environmental Program (UNEP) highlighted an estimated illegal wildlife business worth $3million in a 2015 report [2], the proceeds of which ends up with organized criminal networks. Table 1 presents a list of some critically endangered animal species presently, culled from World Wild Life Fund (WWF) [3]. National Geographic reports that there are only three Northern white rhinos remaining in the world [4]. It would be of great benefit if methods could be devised to help protect these rare species from extinction.

The application of Unmanned Aerial Vehicles to ecology and wildlife is not new. Lesley Evans in his bio-brief [5] highlighted the use of UAVs as a scientific tool for field biologists highlighting that they could carry cameras capable of infrared spectrometry. They can also be used to scare away crop pests and deliver pesticides. Similar discussion could be found in [6] and [7]. In [8] however, a UAV was used to survey mammals in Southern Burkina Faso using an attached camera. The mammals did not react to the UAV flying at 100m altitude. Only elephants were visible from the images obtained from a sample of 7000 while smaller and medium sized mammals remained invisible. The tracking of wildlife has been approached by different authors. WWF reported the use of fixed wing UAVs to track RFID-tagged animals in order to foil poachers in Namibia [9]. In [10], the authors proposed radio tagging where the use of small radio transmitters attached to animals are located using directional antennas. A received-signal-strength (RSS) sensor was designed for a fixed-wing UAV and particle filter was used for localization. The application of UAVs was further extended to the counting and monitoring of animals. Pablo Chamoso et al. [11], in their work, proposed the use of image processing based on convolutional neural networks with a UAV to count and monitor large swarms of livestock. Miguel A. Olivares-Mendez et al. also proposed a solution to the surveillance of animals using quadrotors based on vision processing techniques [12]. The autonomous tracking of marine animals was also reported by William Selby [13]. Visual servoing was employed in [13] for the autonomous tracking of Whales. The method proposed was shown to have lower computational requirements. On the other hand, thermal imaging was used for wildlife monitoring in [14].

In this work, a virtual solution is proposed for the surveillance of Northern white rhinos based on UAV quadrotors capable of hovering unlike fixed-wing aircrafts. A collar with an embedded sensor is attached to the horn of a virtual rhino. It is assumed that with this sensor and strategically placed land based beacons, the range and orientation information of the rhino can be obtained. Using Extended Kalman Filter technique, the localization problem of the rhino is solved. The position coordinates obtained from localization are first sent through a tracking differentiator. The Tracking differentiator (TD) reproduces a smoothed version of the position signals and it's rate of change. Output of the TD is implemented as the trajectory points to be tracked by the quadrotor. For simplification and simulation purpose, the rhino is modelled as a simple Ackerman vehicle wherein different motion trajectories can be simulated. The localization of the Northern White Rhinoceros is simplified based on the assumption that its habitat is a virtual flat field. A beacon node is placed at every edge of a virtual square field habitat while a sensor is placed on the rhino. The beacons are capable of providing range

Table 1 Critically Endangered Species and their Estimated Current Populations

Species	Scientific Name	Population
South China Tiger	*Panthera tigris amoyensis*	0
Northern White Rhino	*Ceratotherium simum cottoni*	3
Amur Leopard	*Panthera pardus orientalis*	60
Javan Rhino	*Rhinoceros sondaicus*	60
Vaquita	*Phocoena sinus*	100

and orientation information of the rhino to a certain degree of accuracy. An approach to estimation of the rhino's position is proposed by using partial-sensing to realize roughly 75 % energy savings. In partial sensing, only one beacon in closest proximity of the rhino is switched "on" out of four. The energy savings here is however counteracted by the power requirements in communication between the beacons, central station that handles switching and information gathering and the quadrotor. On the other hand, there is more power resources available to the quadrotor for the user to attach video surveillance tools. The types of gadgets attached is left to the imagination of the reader. This paper is organized as follows: Section 2 presents the dynamic model of the quadrotor and Rhinoceros motion. In Section 3, the backstepping controller is formulated. Section 4 described the localization problem. Section 5 presents the fusion of all subsystems and parameter optimization. Section 6 contains the summary of results obtained and the conclusion of the research work.

2 QUADROTOR AND RHINO MODEL

2.1 Quadrotor Modeling

The quadrotor model is written in state space form (1) with corresponding state vector representing ϕ, $\dot{\phi}$, θ, $\dot{\theta}$, ψ, $\dot{\psi}$, z, $\dot{z}$, x, $\dot{x}$, y, $\dot{y}$ given as $x_1, x_2, x_3, x_4, x_5, x_6, x_7, x_8, x_9, x_{10}, x_{11}, x_{12}$. Where x_1 is the ϕ-roll angle, x_3 is the θ-pitch angle, x_5 is the ψ-yaw angle, x_7 is the z-altitude state, x_9 is the x-translation and x_11 is the y-translation.

$$\dot{x} = \begin{bmatrix} x_2 \\ U_2 a_6 - a_2 x_4 \Omega_r + a_1 x_4 x_6 + \Delta_a \\ x_4 \\ U_3 a_7 - a_4 x_2 \Omega_r + a_3 x_2 x_6 + \Delta_b \\ x_6 \\ U_4 a_8 + a_5 x_2 x_4 + \Delta_c \\ x_8 \\ g - \frac{U_1}{m}(\cos x_3 \cos x_1) + \Delta_d \\ x_{10} \\ -\frac{U_1}{m}(\sin x_1 \sin x_5 + \sin x_3 \cos x_1 \cos x_5) + \Delta_e \\ x_{12} \\ -\frac{U_1}{m}(\cos x_1 \sin x_3 \sin x_5 - \sin x_1 \cos x_5) + \Delta_f \end{bmatrix} \quad (1)$$

Δ_i represents the aerodynamic drag on the subsystems and are defined as follows; $\Delta_a = -k_{x_2} x_2$, $\Delta_b = -k_{x_4} x_4$, $\Delta_c = -k_{x_6} x_6$, $\Delta_d = -k_{x_8} x_8$, $\Delta_e = -k_{x_{10}} x_{10}$. Similarly, a_i contains the inertia model parameters; $a_1 = \frac{I_{yy} - I_{zz}}{I_{xx}}$, $a_2 = \frac{J_r}{I_{xx}}$, $a_3 = \frac{I_{zz} - I_{xx}}{I_{yy}}$, $a_4 = \frac{J_r}{I_{yy}}$, $a_5 = \frac{I_{xx} - I_{yy}}{I_{zz}}$, $a_6 = \frac{l}{I_{xx}}$, $a_7 = \frac{l}{I_{yy}}$, $a_8 = \frac{1}{I_{zz}}$. m is the mass of the quadrotor and Ω_r is the relative rotor speed defined as:

$$\Omega_r = -\Omega_1 + \Omega_2 - \Omega_3 + \Omega_4$$

where Ω_1 - Ω_4 are rotor speeds characterized by

$$\begin{bmatrix} U_1 \\ U_2 \\ U_3 \\ U_4 \end{bmatrix} = \begin{bmatrix} k_f & k_f & k_f & k_f \\ 0 & -k_f & 0 & k_f \\ k_f & 0 & -k_f & 0 \\ k_m & -k_m & k_m & -k_m \end{bmatrix} \begin{bmatrix} \Omega_1^1 \\ \Omega_2^2 \\ \Omega_3^3 \\ \Omega_4^4 \end{bmatrix} \quad (2)$$

U_1 is the altitude control signal, U_2 is responsible for the roll and U_3 for pitch while U_4 is the required control signal for the desired yaw (heading) angles. k_f and k_m are constants of aerodynamic force and moments respectively. Similarly, $\Delta_a - \Delta_f$ encapsulates undesirable disturbances.

2.2 Rhino Motion Modeling

The model of the rhino was developed in similitude to that of an Ackerman vehicle [15]. The inputs to the model are velocity $V(k) = V$, assumed to be constant when the rhino is taking a stroll and the turning angle $\phi(k)$. The states of interest are the position $x(k)$ and $y(k)$ of the rhino while its bearing is given by $\bar{\omega}(k)$. The sensor states r is the rhino's range from the sensor and θ is it's orientation while δ_t is the time step. Variables $w(k), v(k)$ are the rhino and sensor noise with covariance $Q(k)$ and $R(k)$ respectively. The system thus described is nonlinear of the form (3).

$$\begin{aligned} x(k+1) &= f(x(k), u(k), k) + w(k) \\ z(k) &= h(x(k), k) + v(k) \end{aligned} \quad (3)$$

where x(k+1) and z(k) represent plant and sensor dynamics respectively. The model is given in (4) with states, position $x(k)$, $y(k)$ and bearing $\bar{\omega}(k)$;

$$x(k) = \begin{bmatrix} x(k) + \delta_t V(k) \cos(\bar{\omega}(k) + \phi(k)) \\ y(k) + \delta_t V(k) \sin(\bar{\omega}(k) + \phi(k)) \\ \bar{\omega}(k) + \delta_t V(k) \sin(\phi(k)) \end{bmatrix} + w(k) \quad (4)$$

where $x(k) = [x(k+1)\ y(k+1)\ \bar{\omega}(k+1)]^T$
The model representing the beacons with collar sensor providing range and orientation information is given as:

$$z(k) = \begin{bmatrix} \sqrt{(X - x(k))^2 + (X - x(k))^2} \\ \arctan\left(\frac{Y - y(k)}{X - x(k)}\right) - \phi(k) \end{bmatrix} + v(k) \quad (5)$$

where $z(k) = [r(k), \theta(k)]^T$ are the sensor readings while X and Y is the coordinate of a single beacon. The Jacobian (linearization) of the rhino and sensor models are obtained by differentiation with respect to the state variables:

$$\frac{\partial f}{\partial x} = \begin{bmatrix} 1 & 0 & -\delta_t V(k) \sin(\bar{\omega}(k) + \phi(k)) \\ 0 & 1 & \delta_t V(k) \cos(\bar{\omega}(k) + \phi(k)) \\ 0 & 0 & 1 \end{bmatrix}$$

$$\frac{\partial h}{\partial x} = \begin{bmatrix} \frac{x(k) - X}{d} & \frac{y(k) - X}{d} & 0 \\ \frac{-y(k) - Y}{d^2} & \frac{x(k) - X}{d^2} & -1 \end{bmatrix} \quad (6)$$

3 Backstepping controller

The quadrotor's roll controller is developed based on the roll subsystem ($\phi = x_1$):

$$\begin{aligned} x_1 &= x_2 \\ x_2 &= U_2 a_6 - a_2 x_4 \Omega_r + a_1 x_4 x_6 - k_(x_2) x_2 \end{aligned} \quad (7)$$

An error variable e_1 is defined based on the difference between the desired reference and actual roll ($\phi = x_1$) angle:

$$e_1 = x_{1r} - x_1 \quad (8)$$

A positive definite Lyapunov function is defined in terms of the error variable:

$$V_1(e_1) = \frac{1}{2} e_1^2 \quad (9)$$

If the time-derivative of a Lyapunov function in error variables (V(e)) is negative definite, it implies that the error would decay to

zero which is desirable in Lyapunov-based controller design. Thus the time derivative of the Lyapunov function (9) is

$$\begin{aligned} \dot{V}_1 &= e_1\dot{e}_1 \\ \dot{V}_1 &= e_1(\dot{x}_{1r} - x_2) \end{aligned} \tag{10}$$

x_2 is now regarded as a virtual input on the first subsystem coming from the next subsystem in the feedback plant. Thus let, $x_2 \to \tilde{x}_2$ where $\tilde{x}_2$ is the required value of x_2 chosen so that $\dot{V}_1 \leq -W_1(e_1)$ and $W_1(e_1)$ is chosen as a positive definite function $W_1(e_1) = p_1 e_1^2$ with $p_1 > 0$. Thus:

$$\dot{e}_1 = \dot{x}_{1r} - x_2$$

and therefore

$$\dot{V}_1 = e_1(\dot{x}_{1r} - \tilde{x}_2) \tag{11}$$

choosing $\tilde{x}_2 = \dot{x}_{1r} + p_1 e_1$ guarantees that $\dot{V}_1 = -W_1(e_1)$ which satisfies $\dot{V}_1 \leq -W_1(e_1)$. A new error variable e_2 is defined based on the difference between x_2 and its required value.

$$e_2 = x_2 - \tilde{x}_2 \tag{12}$$

knowing that $\tilde{x}_2 = \dot{x}_{1r} + p_1 e_1$ an substituting into the error equation above:

$$\begin{aligned} e_2 &= x_2 - \dot{x}_{1r} - p_1 e_1 \\ x_2 &= e_2 + \dot{x}_{1r} + p_1 e_1 \end{aligned}$$

Therefore, the Lyapunov equation in equation (11) can be written as:

$$\begin{aligned} \dot{V}_1 &= e_1\dot{e}_1 = e_1(\dot{x}_{1r} - (e_2 + \dot{x}_{1r} + p_1 e_1)) \\ \dot{V}_1 &= -e_1 e_2 - p_1 e_1^2 \end{aligned} \tag{13}$$

$\dot{V}_1$ is always negative definite for $\forall\ e_1, e_2 > 0$. A new Lyapunov function V_2 is defined. V_2 incorporates the second part of the plant while making a case for the appearance of the control input U_2 which needs to be evaluated. Let:

$$V_2 = V_1 + \frac{1}{2}e_2^2$$

The time derivative of V_2 is:

$$\dot{V}_2 = \dot{V}_1 + e_2\dot{e}_2 \tag{14}$$

$$\dot{V}_2 = -e_1 e_2 - p_1 e_1^2 + e_2(\dot{x}_2 - \ddot{x}_{1r} - p_1\dot{e}_1) \tag{15}$$

where $e_2 = x_2 - \dot{x}_{1r} - p_1 e_1$ and $\dot{e}_2 = \dot{x}_2 - \dot{x}_{1r} - p_1\dot{e}_1$. As previously, a second positive definite bounding function augmenting the first is defined

$$W_2(e) = p_1 e_1^2 + p_2 e_2^2 \tag{16}$$

So that $\dot{V}_2(e) \leq -W_2(e)$ and thus:

$$\dot{V}_2 = -e_1 e_2 - p_1 e_1^2 + e_2(\dot{x}_2 - \ddot{x}_{1r} - p_1\dot{e}_) \leq -p_1 e_1^2 - p_2 e_2^2$$

Replacing $\dot{x}_2$ with it's appropriate value from (1), the control input U_2 appears and equation (17) is solved for the value of U_2 that makes $\dot{V}_2 = -p_1 e_1^2 - p_2 e_2^2$ which is always negative definite $\forall\ e_1 e_2 \neq 0$.

$$\begin{aligned} \dot{V}_2 &= -e_1 e_2 - p_1 e_1^2 + e_2(U_2 a_6 - a_2 x_4 \Omega_r + a_1 x_4 x_6 - k_{x_2} x_2 \\ &\quad -\ddot{x}_{1r} - p_1\dot{e}_1) \leq -p_1 e_1^2 - p_2 e_2^2 \end{aligned} \tag{17}$$

The backstepping control input for the roll channel ($x_1 = \phi$) which stabilizes the roll subsystem is thus obtained as (18):

$$\begin{aligned} U_2 = \frac{1}{a_6}(a_2 x_4 \Omega_r - a_1 x_4 x_6 + k_{x_2} x_2 + \ddot{x}_{1r} + \\ p_1\dot{e}_1 + e_1 - p_2 e_2) \end{aligned} \tag{18}$$

Using similar approach, the controllers for the pitch (U_3) yaw (U_4) and altitude (U_1) dynamics respectively are defined as follows:

$$\begin{aligned} U_3 &= \frac{1}{a_7}(-a_4 x_2 \Omega_r - a_3 x_2 x_6 + k_{x_4} x_4 + \ddot{x}_{3r} + \\ &\quad p_3\dot{e}_3 + e_3 - p_2 e_4) \end{aligned} \tag{19}$$

$$\begin{aligned} U_4 &= \frac{1}{a_8}(a_5 x_2 x_4 + k_{x_6} x_6 + \dot{x}_{5r} + p_5\dot{e}_5 + \\ &\quad e_5 - p_6 e_6) \end{aligned} \tag{20}$$

The altitude controller is given as:

$$\begin{aligned} U_1 = \frac{m}{G(\cos x_3 \cos x_1)}(g + k_{x_8} x_8 - \ddot{x}_{7r} - p_7\dot{e}_7 - \\ e_7 + p_8 e_8) \end{aligned} \tag{21}$$

The position subsystem (x and y) represents the under-actuated part of the quadrotor dynamics. A quadrotor has to change its roll and pitch angles to move in the x and y directions. Since stable controllers for the roll and pitch (18)-(19) have been developed, it is intuitive to reverse the system by augmenting the controller such that the roll and pitch dynamics are automatically tuned to drive the quadrotor to the desired x and y positions. A proportional-derivative controller was used for this inner loop control subsystem. Position Controller based on the position subsystem:

$$\begin{aligned} \ddot{x} &= -\frac{U_1}{m}(\sin\phi_d \sin\psi + \cos\phi_d \sin\theta_d \cos\psi) \\ \ddot{y} &= -\frac{U_1}{m}(\cos\phi_d \sin\theta_d \sin\psi - \sin\phi_d \cos\psi) \end{aligned}$$

by small angles approximation $sin(\epsilon) = \epsilon, \cos(\epsilon) = 1$ where ϵ is a small number (preferably $|\epsilon|$ < 20 deg), the position subsystem is simplified to (22):

$$\begin{aligned} \ddot{x} &= -\frac{U_1}{m}(\phi_d \sin\psi + \theta_d \cos\psi) \\ \ddot{y} &= -\frac{U_1}{m}(\theta_d \sin\psi - \phi_d \cos\psi) \end{aligned} \tag{22}$$

$$\begin{bmatrix} -\sin\psi & -cos\psi \\ cos\psi & -\sin\psi \end{bmatrix} \begin{bmatrix} \phi_d \\ \theta_d \end{bmatrix} = \frac{m}{U_1} \begin{bmatrix} \ddot{x} \\ \ddot{y} \end{bmatrix}$$

$$\begin{bmatrix} \phi_d \\ \theta_d \end{bmatrix} = \begin{bmatrix} -\sin\psi & -cos\psi \\ cos\psi & -\sin\psi \end{bmatrix}^{-1} \frac{m}{U_1} \begin{bmatrix} \ddot{x} \\ \ddot{y} \end{bmatrix} \tag{23}$$

and with the proportional-derivative controller:

$$\begin{aligned} \ddot{x} &= k_{px}(x_r - x) + k_{dx}(\dot{x}_r - \dot{x}) \\ \ddot{y} &= k_{py}(y_r - y) + k_{dy}(\dot{y}_r - \dot{y}) \end{aligned} \tag{24}$$

Thus, the ϕ_d and θ_d obtained are used as the desired set points of the roll and pitch subsystems in the already obtained stable backstepping controllers.

4 Extended Kalman Filter

Given a system model of the form:

$$\begin{aligned} x(k+1|k) &= f(x(k|k), u(k), k) + w(k) \\ z(k) &= h(x(k), k) + v(k) \end{aligned} \quad (25)$$

The Extended Kalman filter is applicable by linearizing the plant dynamics. Initial guesses of the states and error covariance need to be chosen for estimation. It is straight forward to take position of the cage or housing as the initial position of the rhino with high certainty. The initial guess has to be close to the true initial values for efficient performance of the nonlinear estimation algorithm [16]. The error covariance is initialized based on prior knowledge and belief but subsequently defined as:

$$P(k+1|k) = \Big(\frac{\partial f}{\partial x}\Big) P(k|k) \Big(\frac{\partial f}{\partial x}\Big)^T + Q(k) \quad (26)$$

The predicted state estimate is given by:

$$x(k+1|k+1) = x(k+1|k) + K(k+1)[z(k)h(x(k+1|k))] \quad (27)$$

with the corresponding error covariance

$$P(k+1|k+1) = P(k+1|k) - K(k+1)S(k+1)K^T(k+1) \quad (28)$$

where the kalman gain is defined as:

$$K(k+1) = P(k+1|k) \Big(\frac{\partial h}{\partial x}\Big)^T S(k+1)^{-1} \quad (29)$$

and

$$S(k+1) = \Big(\frac{\partial h}{\partial x}\Big) P(k+1|k) \Big(\frac{\partial h}{\partial x}\Big)^T + R(k+1) \quad (30)$$

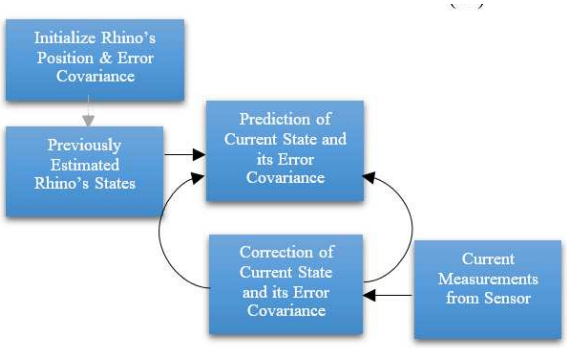

Fig. 1: EKF Estimation Cycle

5 System Application

The backstepping controllers are applied to their respective subsystems. In total, there are eight backstepping control parameters to be tuned and two PD control parameters. The altitude, roll, pitch and yaw subsystems are to track the rhino's position coordinates x(k) and y(k) by changing quadrotor's translational set-points. The rhino's x and y position coordinate is passed through individual tracking differentiators [17], [18]:

$$\begin{aligned} \dot{\tilde{x}}_1 &= \tilde{x}_2 \\ \dot{\tilde{x}}_2 &= -1.76\bar{R}\tilde{x}_2 - \bar{R}^2(\tilde{x}_1 - u) \end{aligned}$$

$\tilde{x}_1$ represents the tracked x or y rhino's coordinate, $\tilde{x}_2$ is the rate of change of the coordinates while u is the tracked signal input (x or y) to the tracking differentiator. Thus, the position controller is set for tracking the rhino with set-points $x_d = \tilde{x}_1$ and $\dot{x}_d = \tilde{x}_2$ and same is repeated the y coordinate. The tracking differentiator (31) dampens the quadrotor's reaction to the stochastic nature of the tracked trajectory as shown in Figure 11. The system is simulated with four beacons having similar characteristics. J. Leonard has treated robot localization using geometric beacons in his work [19]. In this work, partial-sensing for localization is used instead of full- sensing. The full-sensing case is also referred to as the inefficient case because all four sensors have to be powered 'on' while the partial sensing is referred to as the efficient case because only one of four sensors is 'on'. In full-sensing, estimation is performed using all beacons switched on and measuring whereas partial sensing involves the activation of the beacon in closest proximity to the rhino. Hypothetically, information obtained is sent to a central processing station for estimation. When out of range of the first beacon, the next closest beacon in the grid of four beacons performs the localization of the rhino while others are set to hibernate mode. This is for energy savings and the switching is done by the central station automatically. Parameter optimization is very crucial for any tuning problem. Numerous algorithms have been developed for optimization and utilized in a cornucopia of applications; even outside the control field. In [20], the particle swarm algorithm was applied for the optimization of mobile robot controller while [21] applied genetic algorithms to tune PID controllers. Optimization can be applied online (gains are dynamically fitted during process loop) or offline (static gains obtained are used in the process loop). The objective function is set to minimize or maximize a cost function. The use of evolutionary algorithms to optimize system parameters is widespread and often requires a tedious development of code to implement the algorithms. In this work, Gradient Descent-Sequential Quadratic Programming combined with parallel computing was used to optimize the controller parameters for fast response and minimized offshoot.

6 SIMULATION AND RESULTS

The simulation was done using Matlab. The rhino's position coordinates from the Extended Kalman filter is sent to the quadrotor's position controller for tracking. The initialized parameters of the rhino's model include: mean of noise disturbance; μ, variance of noise in x; σ_x, variance of noise in y; σ_y, variance of noise along orientation $\bar{\omega}$; $\sigma_{\bar{\omega}}$. The variance of sensor's measurement noise in range r; σ_r, variance of noise in bearing θ; σ_θ and δ_t the time step. The error covariance Q , P and R are diagonal matrices with diagonal elements as described in Table 2. where $q = (\sigma_x^2, \sigma_y^2, \sigma_{\bar{\omega}}^2)$,

Table 2 System Parameters

Param	Value	Param	Value	Param	Value
g	9.81	J_r	0.006	k_{x_i}	0.3729
l	0.23	m	1.0	σ_x	0.3729
I_{xx}	0.075	p_1	11.5	σ_y	0.05
I_{yy}	0.0075	p_2	8.4	$\sigma_{\bar{\omega}}$	$\frac{\pi}{180}$
I_{zz}	0.013	p_3	8.0	σ_r	0.5
K_{px}	4.9	p_4	7.5	σ_θ	$\frac{2\pi}{180}$
K_{py}	4.9	p_5	13.62	Q	diag(q)
K_{dx}	7.3	p_6	13.54	R	diag(r)
K_{dy}	8.3	p_7	1.54	P	diag(p)
		p_8	3.49	σ_t	1

$r = (\sigma_r^2, \sigma_\theta^2)$, $p = (10^{-4}, 10^{-4}, 10^{-6})$, $R = 10$, $\mu = 0$.

The results in this section include graphs of the true rhino motion (corrupted with noise) and estimated rhino motion, range and the MSE errors in range estimation for a circular motion trajectory. As shown in Figure 2, the rhino makes a circular path while the localization system maps its estimated trajectory using partial sensory information. The estimated range covered by the rhino is shown in

Figure 3. Figure 4 is the same rhino motion localized using full sensing. The localization is more accurate because more sensors are used. In Table 3, the mean squared error is used to compare the partial and full sensing modes of the localization system. It is intuitive that full sensing gives better localization results at the detriment of higher energy consumption needed to power all sensors at the same time while on the other hand, partial sensing mode gives a fairly good localization result with less energy requirement as observed in the localization results and MSE values in Figures 2-5.

Table 3 Error in Range Estimation

	Full Sensing, (Inefficient)	Partial Sensing, (Efficient)
MSE	0.0273	0.1772

7 Discussion and Conclusion

Increasing the number of active sensors or beacons improves the estimation and this can be observed from the mean square error (MSE) Table 3. It is also clear from the rhino position plots (Figure 2 against Figure 4) that with more sensors, the estimation results are smoother, however, this comes at the cost of switching all the sensors 'on' thus higher power consumption. The most important trade-off for this application is in power consumption, and it is easy to observe that by partial sensing, approximately 75% energy savings is achievable (since only one sensor is active out of four). The choice of partial sensing is justified because the system does not require stringent accuracy and precision for tracking the rhino. Specific error magnitudes can be tolerated. The tracking differentiator smoothens the rhino's noisy trajectory for the backstepping controller. The backstepping controller with optimized parameters track the rhino's coordinates. In the first simlation, Figures 6-7 show the quadrotor accurately homing the Rhino. Figure 8 shows the 3D plot of the quadrotor-rhino tracking process. The quadrotor takes-off to an altitude of 8m and thereafter tracks the Rhino's location. In the second simulation, Figures 10-15, the quadrotor tracks the Rhino's circular path. Figure 10 and 11 shows the quadrotor and rhino x-y coordinates with respect to time. In Figure 12 and 13, the effect of the Tracking differentiator on the noise localization signals can be observed. The tracking differentiator (TD) acts as a form of filter while at the same time introducing time delay. This time delay affects the accuracy of the tracking system (Figure 10-11). Noisy signals get amplified after derivative action and the TD also helps in attenuating this effect as shown in Figure 13.

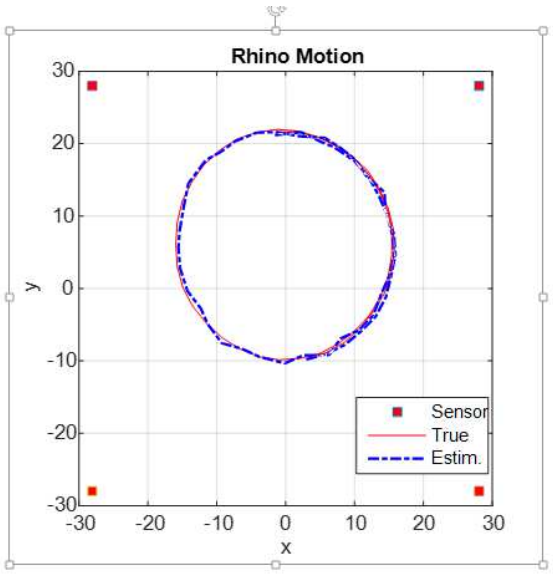

Fig. 2: Estimation of Rhino's Position with Partial Sensing

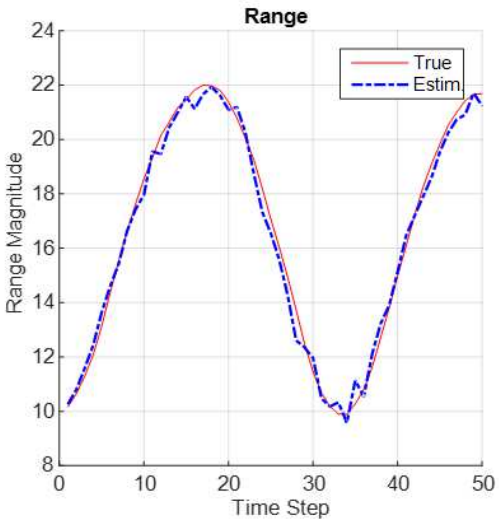

Fig. 3: Rhino's Range with Partial Sensing

8 References

[1] G. Cai, J. Dias, and L. Seneviratne, "A Survey of Small-Scale Unmanned Aerial Vehicles: Recent Advances and Future Development Trends," Unmanned Systems, vol. 2, no. 2, pp. 175âĂŞ199, 2014.
[2] S. Zorba, "Experts background report on illegal exploitation and trade in natural resources benefitting organized criminal groups and recommendations on MONUSCO's role in fostering stability and peace in eastern DR Congo," 2015.
[3] "World Wild Life." [Online]. Available: http://www.worldwildlife.org/.
[4] B. C. Howard, "National Geographic," 2015. [Online]. Available: http://news.nationalgeographic.com/2015/11/151123-nola-northern-white-rhino-dies-conservation-animals/.
[5] L. E. Ogden, "Drone Ecology," BioScience, vol. 63, no. 9, pp. 776âĂŞ776, 2013.
[6] D. Chabot and D. M. Bird, "Wildlife research and management methods in the 21st century: Where do unmanned aircraft fit in 1," Journal of Unmanned Vehicle Systems, vol. 3, no. 4, pp. 137âĂŞ155, 2015.
[7] J. C. Hodgson and L. P. Koh, "Best practice for minimising unmanned aerial vehicle disturbance to wildlife in biological field research," Current Biology, vol. 26, no. 10, pp. R404âĂŞR405, 2016.
[8] P. B. Cederic Vereulen, Philippe Lejeune, Jonathan Lisein, Prosper Sawadogo, "Unmanned Aerial Survey of Elephants," PLOS One, vol. 8, no. 2, 2013.
[9] J. Edwards, "World Wildlife Fund Uses RFID to Foil Poachers," RFID Journal, Apr-2014.
[10] F. K??rner, R. Speck, A. H. G??kto??an, and S. Sukkarieh, "Autonomous airborne wildlife tracking using radio signal strength," IEEE/RSJ 2010 International Conference on Intelligent Robots and Systems, IROS 2010 - Conference Proceedings, pp. 107-112, 2010.
[11] A. G. Pablo Chamoso, William Raveane, Victor Parra, "UAVs Applied to the Counting and Monitoring of Animals," Advances in Intelligent Systems and Computing, vol. 291, pp. 71-80, 2014.
[12] Y. Song, B. Xian, Y. Zhang, X. Jiang, and X. Zhang, "Towards autonomous control of quadrotor unmanned aerial vehicles in a GPS-denied urban area via laser ranger finder," Optik - International Journal for Light and Electron Optics, vol. 126, no. 23, pp. 3877-3882, 2015.

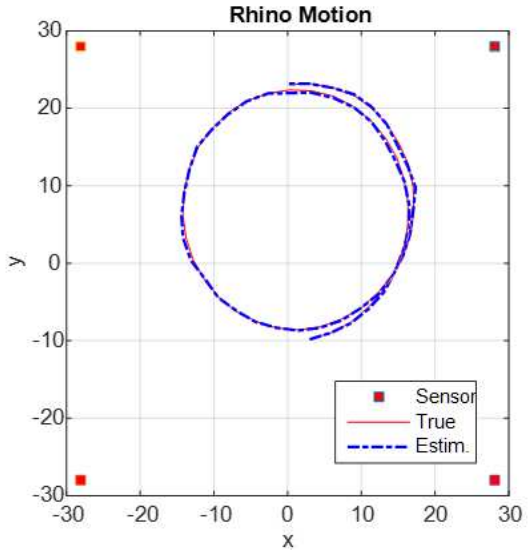

Fig. 4: Estimation of Rhino's Position with Full Sensing

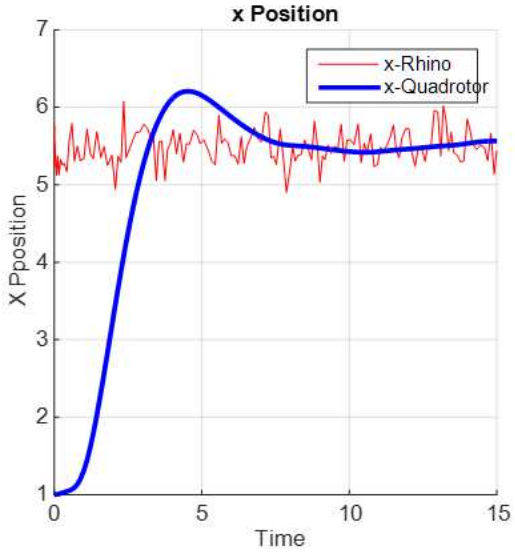

Fig. 6: Quadrotor Tracking Rhino in x-Direction

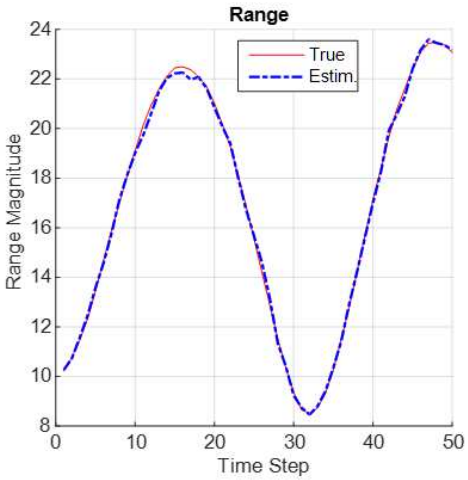

Fig. 5: Rhino's Range with Full Sensing

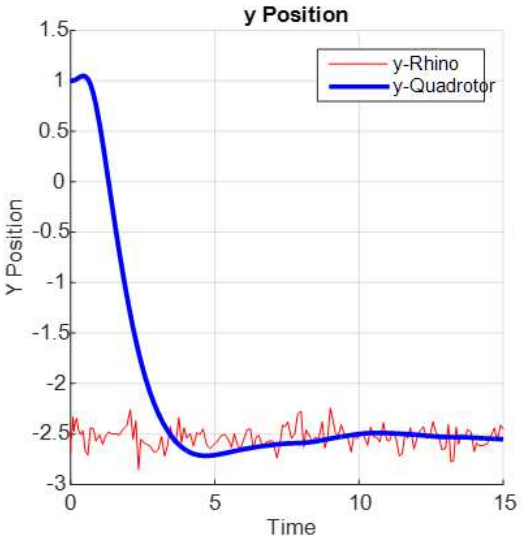

Fig. 7: Quadrotor Tracking Rhino in y-Direction

[13] W. Selby, P. Corke, and D. Rus, "Autonomous Aerial Navigation and Tracking of Marine Animals," in Proceedings of Australasian Conference on Robotics and Automation, 2011, pp. 7-9.
[14] L. F. Gonzalez, G. A. Montes, E. Puig, S. Johnson, K. Mengersen, and K. J. Gaston, "Unmanned aerial vehicles (UAVs) and artificial intelligence revolutionizing wildlife monitoring and conservation," Sensors (Switzerland), vol. 16, no. 1, 2016.
[15] P. Corke, Robotics, Vision and Control: Fundamental Algorithms in Matlab. 2013.
[16] E. L. H. and J. B. Rawlings, "A Critical Evaluation of Extended Kalman Filtering and Moving Horizon Estimation," Texas-Wisconsin, 2003.
[17] J. Han, "From PID to Active Disturbance Rejection Control," IEEE Transactions on Industrial Electronics, vol. 56, no. 3, pp. 900-906, 2009.
[18] Y. Li, Z. Chen, M. Sun, Z. Liu, Q. Zhang, Y. Li, ÃĄ. Z. Chen, ÃĄ. M. Sun, and ÃĄ. Z. Liu, "ADRC Based Attitude Control of a Quad-rotor Robot."
[19] J. J. Leonard and H. F. Durrant-Whyte, "Mobile robot localization by tracking geometric beacons," IEEE Transactions on Robotics and Automation, vol. 7, no. 3, pp. 376-382, 1991.
[21] O. Elshazly, Z. Zyada, A. Mohamed, and G. Muscato, "Optimized Control of Skid Steering Mobile Robot with Slip Conditions," in IEEE International Conference on Advanced Intelligent Mechatronics (AIM), 2015, pp. 959-964.
[21] J. Cao and B. Cao, "Design of Fractional Order Controllers Based on Particle Swarm Optimization," in 1ST IEEE Conference on Industrial Electronics and Applications, 2006, pp. 1-6

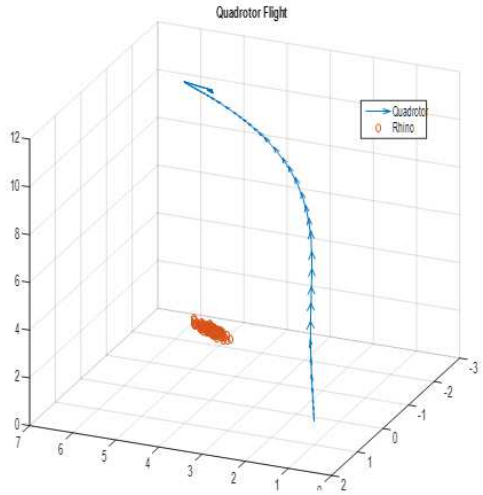

Fig. 8: Quadrotor tracking Rhino in 3D

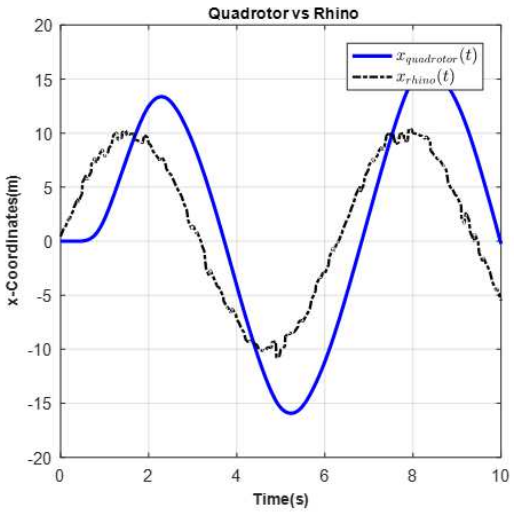

Fig. 11: Quadrotor and Rhino x-position coordinates

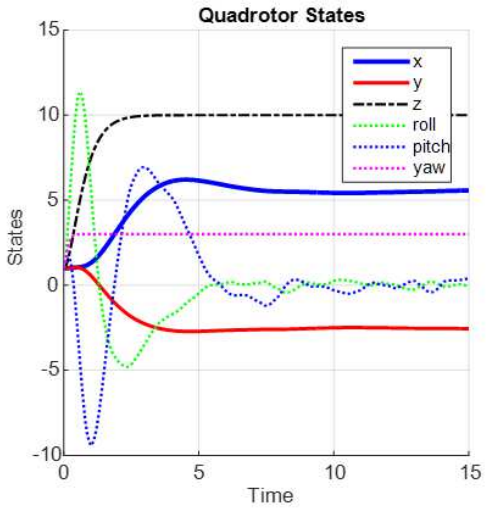

Fig. 9: Other controlled Quadrotor's States

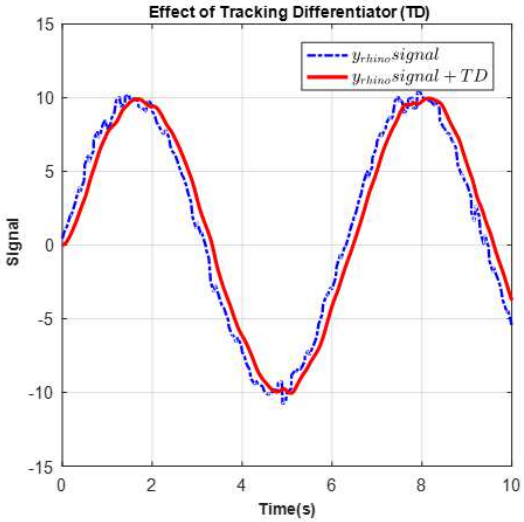

Fig. 12: Effect of Tracking differentiator on Rhino position signals

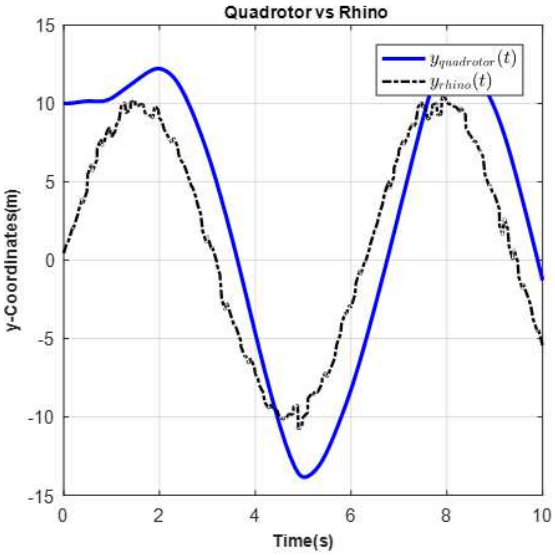

Fig. 10: Quadrotor and Rhino y-position coordinates

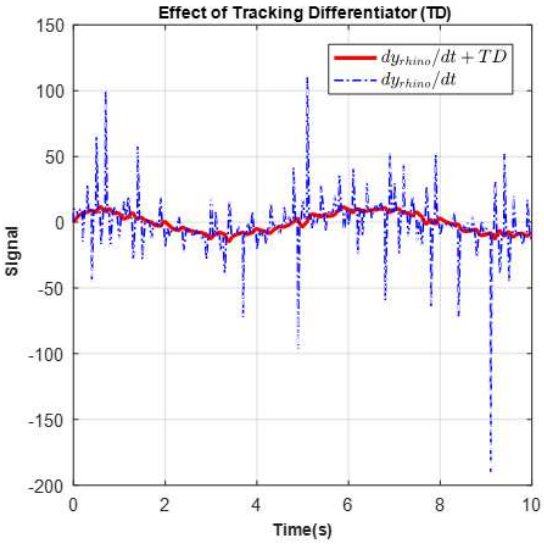

Fig. 13: Effect of Tracking differentiator on the rate of change Rhino position signals

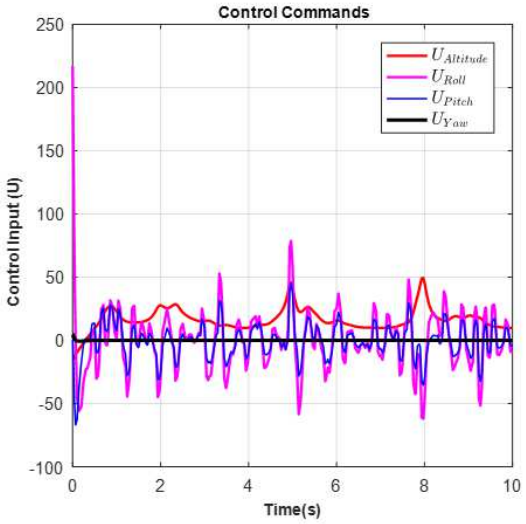

Fig. 14: Quadotor control signals

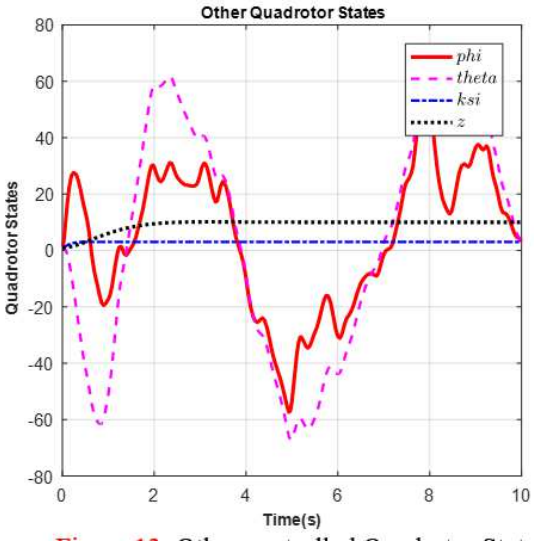

Fig. 15: Other controlled Quadrotor States